

Development 134, 4507 (2007) doi:10.1242/dev.017343

folded gastrulation, cell shape change and the control of myosin localization

Rachel E. Dawes-Hoang, Kush M. Parmar, Audrey E. Christiansen, Chris B. Phelps, Andrea H. Brand and Eric F. Wieschaus

There was an error published in *Development* **132**, 4165-4178.

An acceptance date in 2006 was mistakenly listed. The acceptance date should have read 13 June 2005.

We apologise to the authors and readers for this mistake.

folded gastrulation, cell shape change and the control of myosin localization

Rachel E. Dawes-Hoang^{1,*}, Kush M. Parmar^{1,2}, Audrey E. Christiansen³, Chris B. Phelps⁴, Andrea H. Brand⁴ and Eric F. Wieschaus¹

¹Department of Molecular Biology, Howard Hughes Medical Institute, Princeton University, NJ 08544, USA

²Harvard Medical School, 25 Shattuck Street, Boston, MA 02115, USA

³Department of Biological Sciences, Stanford University, CA 94305

⁴Wellcome Trust/Cancer Research UK Gurdon Institute and Department of Anatomy, University of Cambridge, Cambridge CB2 1QN, UK

*Author for correspondence (e-mail: rhoang@haverford.edu)

Accepted 13 June 2006

Development 132, 4165–4178

Published by The Company of Biologists 2005

doi:10.1242/dev.01938

Summary

The global cell movements that shape an embryo are driven by intricate changes to the cytoarchitecture of individual cells. In a developing embryo, these changes are controlled by patterning genes that confer cell identity. However, little is known about how patterning genes influence cytoarchitecture to drive changes in cell shape. In this paper, we analyze the function of the *folded gastrulation* gene (*fog*), a known target of the patterning gene *twist*. Our analysis of *fog* function therefore illuminates a molecular pathway spanning all the way from patterning gene to physical change in cell shape. We show that secretion of Fog protein is apically polarized, making this the earliest polarized component of a pathway that ultimately drives myosin to the apical side of the cell. We demonstrate that *fog* is both necessary and sufficient to drive apical myosin localization through a mechanism involving activation of

myosin contractility with actin. We determine that this contractility driven form of localization involves RhoGEF2 and the downstream effector Rho kinase. This distinguishes apical myosin localization from basal myosin localization, which we find not to require actinomyosin contractility or FOG/RhoGEF2/Rho-kinase signaling. Furthermore, we demonstrate that once localized apically, myosin continues to contract. The force generated by continued myosin contraction is translated into a flattening and constriction of the cell surface through a tethering of the actinomyosin cytoskeleton to the apical adherens junctions. Our analysis of *fog* function therefore provides a direct link from patterning to cell shape change.

Key words: *Drosophila*, Myosin, Gastrulation, Fog, Morphogenesis, Rho-kinase, RhoGEF, Arm

Introduction

All embryos undergo an elaborate series of morphogenetic movements to produce their final shape and form. Underlying these global movements are intricate changes in the cytoarchitecture of individual cells. When studying these changes within the context of a developing embryo, the genes involved often fall into two broad categories: patterning genes that confer cell identity (such as tissue specific transcription factors) and genes encoding subcellular components (such as cytoskeletal proteins). Understanding how patterning genes interface with cytoskeletal components to control cell shape is central to understanding the molecular basis of morphogenesis. However, very little is known about this process.

A rare opportunity to bridge these categorizations is offered by *folded gastrulation* (*fog*) – a gene involved in *Drosophila* gastrulation. Mutations in *fog* disrupt the movement of mesodermal and endodermal precursor cells into the interior of the embryo (Costa et al., 1994; Oda and Tsukita, 2001). *fog* is not itself a patterning gene, as cell fates are unaltered in *fog* mutants, but *fog* is a direct target of a well described patterning gene, *twist* (Costa et al., 1994). In addition, *fog* encodes a

novel protein that is thought to be the ligand for a signaling cascade that controls changes in cell shape. *fog* may therefore function in morphogenesis by interfacing between the patterning gene *twist* and the machinery that produces cell shape change.

fog protein is required for the earliest visible changes in cell shape that mark the onset of gastrulation. First, the prospective mesodermal cells on the ventral side of the embryo flatten and then constrict their apical surface. This shifts the cells towards the interior of the embryo in a structure called the ventral furrow. In *fog* mutant embryos, these cell shape changes are disorganized and proceed in an uncoordinated manner (Costa et al., 1994). Second, similar cell shape changes initiate internalization of the prospective endoderm on the dorsal posterior surface of the embryo (the posterior midgut primordium). In *fog* mutants these cell shape changes are blocked in all but a few cells. Furthermore, a heat-shock-activated form of *fog* has been shown to elicit the apical flattening of cells in other areas of the embryo (Morize et al., 1998). *fog* therefore plays an important role in controlling the flattening and constriction of the apical surface of cells and is

the primary pathway controlling these cell shape changes in the posterior midgut primordium, whereas a second parallel pathway additionally contributes to these cell shape changes in the ventral furrow. In all these studies *fog* function has been analyzed with respect to the outward appearance of cells. Nothing is known about the molecular remodeling of the cytoarchitecture that must underlie *fog* function.

Fragments of a pathway have started to emerge for the function of *fog* during gastrulation. Embryos lacking the gene product *concertina* (*cta*) show the same disruptions to ventral furrow and posterior midgut formation as seen in *fog* mutants (Parks and Wieschaus, 1991). Furthermore, *cta* has been positioned genetically downstream of *fog* as the effects of a heat-shock-activated form of *fog* are blocked in *cta* mutants and conversely, activated *cta* has effects that are independent of *fog* (Morize et al., 1998). *cta* is known to encode a G-protein alpha subunit of the $G_{\alpha 12/13}$ class. In addition to its own role in the *fog* pathway, *cta* therefore also implicates a role for an as yet unidentified G-protein-coupled receptor. Another gene that disrupts both ventral furrow and posterior midgut formation is *RhoGEF2*, a guanine nucleotide exchange factor that promotes Rho activation and thus also implicates Rho signaling in this process (Barrett et al., 1997; Hacker and Perrimon, 1998). *RhoGEF2* mutants have been shown to be able to interact genetically with a *fog* transgene during early embryonic development (Barrett et al., 1997). However, the ventral furrow phenotype of *RhoGEF2* mutants affects all cells and is therefore much more severe than that of *fog* and *cta* mutants. The way in which the *fog* and *RhoGEF2* pathways interact therefore remains unclear and the relevant downstream signaling components are unknown.

A likely target of the *fog* pathway is non-muscle myosin II (herein referred to as myosin). Myosin is expressed at the right time and place to be involved (Young et al., 1991) and removal of *RhoGEF2* lowers myosin levels at gastrulation (Nikolaidou and Barrett, 2004), though the extent and significance of this disruption is not clear. Furthermore, myosin is known to play an important role in driving many cell shape changes in a wide variety of organisms. One of the best understood of all myosin-based processes is cytokinesis. During cell division, myosin localizes to the cleavage furrow, an assembly of proteins responsible for physically separating newly formed daughter cells. Myosin is thought to function in this process by contributing force in a contractile actin-myosin ring, though much remains to be understood about how this force is coupled to the physical changes in cell shape (Glotzer, 2001; Wang, 2001). The ability of myosin to function as an actin-based motor that provides contractile force is also thought to underlie the role of myosin in many other morphogenetic processes. However, the full range of myosin function is likely to be more complicated, with reports of myosin also involved in downregulating adherens junctions and serving as a spatial cue for cell wall formation during fission yeast cell division (Rajagopalan et al., 2003; Sahai and Marshall, 2002). Myosin may therefore contribute to *Drosophila* gastrulation in a number of different ways.

Consistent with its involvement in a wide range of morphogenetic processes, myosin is also widely expressed. Therefore, in the context of a developing organism, myosin functions in multiple different processes sometimes within the very same cell. As *Drosophila* gastrulation initiates myosin

localization is highly dynamic, being lost from the basal side of mesodermal cells, where it functioned during cellularization, and accumulating apically (Royou et al., 2004; Young et al., 1991) (this study). Therefore, little is known about the specific role of myosin in gastrulation and more generally about how different myosin-based processes, such as cellularization and ventral furrow formation, are related to one another during development. To begin to address these issues, it becomes important to understand the precise dynamics, localization and regional activities of myosin within individual cells over time.

In this paper, we address many of these issues through our analysis of *fog* function. We find that *fog* signal is apically polarized and that this in turn directs the apical localization of myosin. We show that the mechanism driving this apical localization of myosin requires interaction/contractility with actin, distinguishing it from the mechanism driving myosin to the basal side of the same cells. Furthermore, we demonstrate that *fog* is both necessary and sufficient for localization of myosin apically, and that this pathway of myosin activation requires *RhoGEF2* and the downstream effector Rho kinase. Finally, we show that once localized apically, myosin continues to contract and the resulting force is translated into physical changes at the cell surface through a tethering of the actin-myosin cytoskeleton by apical adherens junctions. We therefore provide a mechanism of *fog* function that takes us all the way from the patterning gene *twist*, to physical changes in cell shape at the onset of gastrulation.

Materials and methods

Drosophila strains and genetics

Line *mat67;mat15* is *mat α 4-GAL-VP16* (Hacker and Perrimon, 1998) with inserts homozygosed on II and III. The *sqhGFP* stock is *y w sqh^{AW3} cv; [sqh-gfp¹²]* (Royou et al., 2004). *Fog* stocks are *y w fog¹¹⁴/FM7[ftzLacZ]; In(1)sc⁸Df(1)mal¹² B/y⁺Ymal/C(1)Dx. fog¹¹⁴* is FlyBase *Df(1)fog-1* (Perrimon et al., 1989) and deletes the entire *fog*-coding sequence (Costa, 1994). *shibire^{ts}* is FlyBase *shibire-1*. Oregon R was used as wild type.

Germline clones were produced from the following crosses using standard techniques (Chou and Perrimon, 1992).

Arm: *arm^{043A01} FRT¹⁰¹/FM6 x ovo^{D1} FRT¹⁰¹/Y; hs-flp 138* produced heat shocked *arm^{043A01} FRT¹⁰¹/ovo^{D1} FRT¹⁰¹* females used to collect embryos (Tolwinski and Wieschaus, 2001).

DRhoGEF2: *y w hs-flp;FRT42B^{G13} DRhoGEF2^{1.1}/CyO* virgin females \times *FRT42B^{G13} ovoD1/CyO* males produced heat shocked *FRT42B^{G13} DRhoGEF2^{1.1}/FRT42B^{G13} ovoD1* females that were crossed to *w* males to collect embryos (Barrett et al., 1997).

Drok alleles (Winter et al., 2001) were used to make the following stocks and crosses: *w rok^{1or2} FRT^{18D}/FM7 \times ovo^{D2} FRT^{18D}/Y; hs-flp138* produced heat shocked *w rok^{1or2} FRT^{18D}/ovo^{D2} FRT^{18D}* females from which embryos were collected.

UAS*fog* expressing embryos are from *mat67;mat15* virgins \times UAS*fog* males. Three UAS*fog* lines were used: UAS*fog⁶* (III), UAS*fog¹²* (II) and UAS*fog¹⁸/TM3Ser*. UAS*snullo*-expressing embryos are from *mat67;mat15* virgins \times UAS*snullo^{N39}* males (Hunter et al., 2002). Embryos expressing UAS*mYFP-myosin II^{DN}* are from *mat67;mat15* virgins \times *w; UAS mYFP-myosin II^{DN}* males to produce *w; mat67/UAS mYFP-myosin II^{DN}; mat15/+* virgins backcrossed to *w; UAS mYFP-myosin II^{DN}* to collect embryos.

Embryology, histology and image analysis

All embryos were heat-methanol fixed (Muller and Wieschaus, 1996) except those stained with anti-GFP or anti-Fog antibody, which were

formaldehyde fixed (Zallen and Wieschaus, 2004). SEM analysis was as described previously (Morize et al., 1998). Stained embryos were cross-sectioned by hand in 70% glycerol/PBS (using a 26-gauge hypodermic needle), mounted in Aquapolymount (Polysciences, Warrington, PA) and imaged using a Zeiss LSM-510 confocal microscope (Thornwood, NY).

Reagents used were Hoechst 33342 (Molecular Probes), rabbit anti-Myosin II antibody (1:1250, gift of C. Field), sheep anti-Dorsal antibody (1:500, gift of R. Stewart), mouse anti-Armadillo (1:50, N2-7A1 Developmental Studies Hybridoma Bank, DSHB), mouse anti-Neurotactin (1:10, BP106 from DSHB), guinea pig anti-Runt (1:500, gift of C. Alonso and J. Reinitz) and rabbit anti-GFP (1:2000, Torey Pines). Primary antibodies were detected with Alexa-conjugated secondary antibodies (Molecular Probes). Anti-Fog antibody was produced from a fusion of 6×His, followed by three novel residues, then residues 28 to 303 of *fog* cDNA, then six novel residues. This protein was purified and injected into rabbits. Sera were purified using protein-A-conjugated beads.

Myosin intensity was measured in embryos stained for myosin II and cut by hand into cross-sections. Intensity measurements were taken from the monochrome myosin channel of confocal images, using IPLab software to average pixel intensities along a hand-drawn line on the cellularization front (basal) or apical edge of the embryo (apical) over 10 cell widths. Measurements were taken on both ventral and lateral sides of the embryo and normalized relative to the background pixel intensity (inside nuclei). Each sample contained measurements from at least 100 cells including at least five different embryos.

Myosin dynamics in *fog* mutants: *fog*¹¹⁴ females were crossed to *sqhGFP* males. F1 females carrying both *fog*¹¹⁴ and *sqhGFP* were backcrossed to the *sqhGFP* stock producing both *fog* mutant and control embryos expressing *sqhGFP*. Time-lapse movies were taken using confocal microscopy with images collected every 30 seconds. *fog* mutants were identified by emergence of the *fog* phenotype.

Heat-shock inactivation of *shibire*^{ts}: embryos were collected for 1 hour, allowed to age, dechorionated and transferred to a damp piece of paper towel that was placed on a 35°C heat block for 30 minutes, then fixed for 25 minutes in a 50:50 mixture of 4% formaldehyde in 0.1 M PIPES, 2 mM EGTA, 1 mM MgSO₄ (pH 6.9) and heptane.

Constructs

pUAST-mYFP-myosin-II^{DN}

The central region of myosin II-coding region was PCR amplified from pBS-Zipper (Kiehart et al., 1989) (gift from D. Kiehart), to introduce a *KpnI* site and a glycine linker, and to maintain the *XhoI* site. In a separate reaction, the myosin N terminus was removed from pBS-Zipper by *XhoI* digestion and self-ligation to give pBS-myosin-II-C-terminus. The PCR *KpnI-XhoI* central myosin fragment was inserted into the *KpnI/XhoI*-digested pBS-myosin-II-C-terminus backbone, to create myosin-II^{DN}. This construct contains a dominant-negative form of myosin II, with the head removed at precisely the same point as an equivalent *Dictyostelium* myosin II^{DN} [head-neck junction: amino acid 831 in *Drosophila* (QWWR) and position 809 in *Dictyostelium* (PWWK)] (Burns et al., 1995; Zang and Spudich, 1998). mYFP (Haseloff, 1999) (gift from J. Haseloff) was PCR amplified to introduce *KpnI* and *NotI* sites. The *KpnI* cut mYFP PCR product was inserted into *KpnI* cut pBS-myosin-II^{DN} and correct orientation of the insert selected by position of the *NotI* site. A *NotI*-mYFP-myosin-II^{DN}-*NotI* cassette was excised from pBS and inserted into *NotI*-digested pUAST (Brand and Perrimon, 1993). The correct orientation of the insert was selected by position of the *XhoI* site. This produced the construct pUAST-mYFP-myosin-II^{DN}.

pUAST-fog

Full-length *fog* cDNA was obtained from plasmid pB26H (Costa et al., 1994) by digestion with *NheI* and purification of the *fog*-

containing fragment. pUAST (Brand and Perrimon, 1993) was digested with *XbaI* and ligated with the compatible *NheI* ends of the *fog* fragment. Correct orientation of the insert was screened by PCR.

Transgenic flies were generated using standard techniques (Barros et al., 2003).

Results

fog as a signal for apical myosin localization

We began our investigation of *fog* function with an analysis of *fog* protein distribution within the cells of the ventral furrow and posterior midgut. In both cases we find that *fog* protein is present in a characteristically punctate pattern and that the protein is distributed unevenly within the cells (Fig. 1A-C). The distribution of *fog* protein is polarized with more *fog* puncta present on the apical compared with the basal side of the cells. This punctate staining is consistent with the localization of signaling molecules to vesicles involved in both signal production and reception (Gonzalez-Gaitan, 2003). To investigate this possibility further, we looked at the distribution of *fog* protein in embryos carrying a temperature-sensitive mutation in the gene *shibire*, which encodes the *Drosophila* homolog of dynamin. At the non-permissive temperature, this mutation blocks endocytosis, and exocytosis is also compromised (Chen et al., 1991; Ramaswami et al., 1994). When embryos are shifted to the non-permissive temperature during early gastrulation (earlier shifts severely disrupt the process of cellularization) the *fog* protein is already being made and some protein may already be undergoing endocytosis. However, the localization of *fog* protein in these embryos is still clearly disrupted, with much less punctate staining and a decrease in apical polarization (Fig. 1D,E). This suggests that the punctate staining of *fog* protein in normal embryos may arise from localization to vesicles derived through endocytosis, and this supports the hypothesis that *fog* encodes a secreted protein. The apical polarization of Fog protein therefore raises the possibility that apical secretion and reception of *fog* signal may provide a mechanism for restricting *fog* function to the apical side of the cell.

To understand the molecular basis of the control of the cytoskeleton by *fog*, we have investigated changes in myosin II dynamics in *fog* mutant embryos. Analysis of myosin dynamics is easiest in the posterior midgut where *fog* is the primary pathway controlling cell constriction and the geometry of the egg enables visualization of a myosin lightchain-GFP fusion (*sqhGFP*) in time-lapse movies of living embryos. During gastrulation myosin localizes to the apical side of cells throughout the posterior midgut primordium of control embryos (Fig. 1G). However, in *fog* mutant embryos of the same age, the apical localization of myosin is severely disrupted and is restricted to just a few cells underlying the pole cells (Fig. 1I). Analysis of myosin localization in fixed embryos also reveals a disruption to apical localization, both in the posterior midgut and the ventral furrow of *fog* mutants. This is consistent with previous data showing that myosin is also disrupted in *cta* mutants (Nikolaidou and Barrett, 2004). In the ventral furrow only a subset of cells (39%, *n*=62) localize myosin apically in *fog*¹¹⁴ mutant embryos (Fig. 1H,J). The *fog*¹¹⁴ allele is an RNA null (see Materials and methods). The patchiness of this defect in the ventral furrow of *fog*¹¹⁴ mutants therefore probably reflects the redundancy with additional

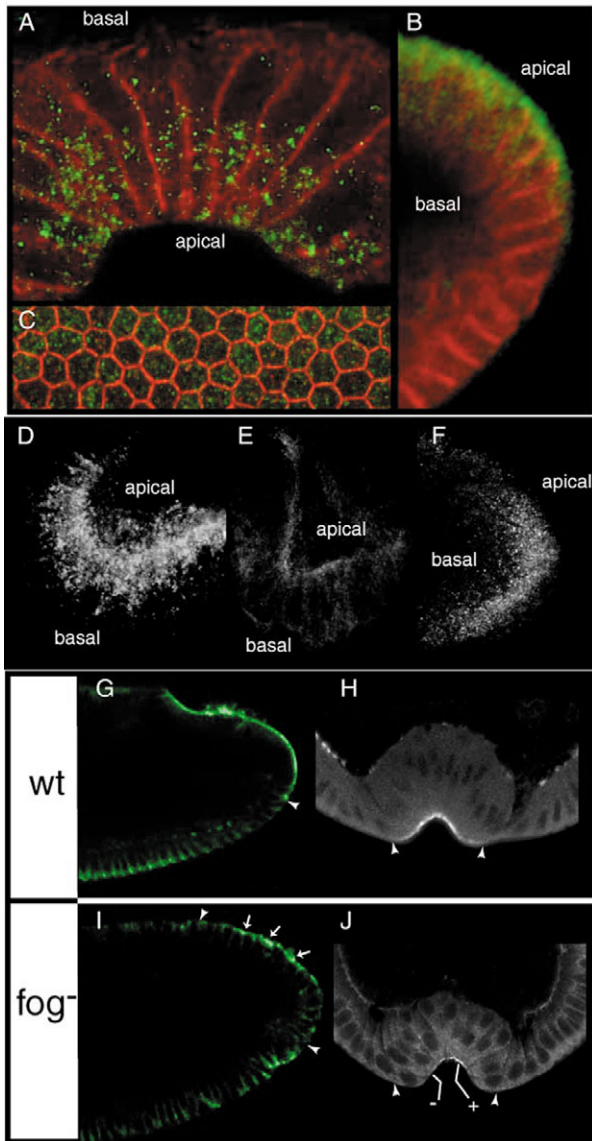


Fig. 1. *folded gastrulation* and myosin localization. (A-C) Antibody staining for *fog* protein (green) and cell outlines (*Nrt*, red) in cross-section of ventral furrow (A), sagittal section of posterior midgut (B) and apical surface of ventral cells (C). There is punctate *fog* staining and localization towards the apical half of the cells. (D-F) Antibody staining for *fog* protein in the region of the posterior midgut in control *shibire^{ts}* embryos kept at the permissive temperature (D), in *shibire^{ts}* embryos shifted to the non-permissive temperature at gastrulation (E), and in embryos from *Rho-kinase* germline clones (F). Punctate staining and apical concentration of *fog* protein is reduced when endocytosis is blocked using the non-permissive *shibire^{ts}* but is maintained in *Rho-kinase* embryos despite the failure of the latter to form a posterior midgut invagination. (G,I) Frames from time-lapse movies of *sqhGFP*-expressing embryos 13 minutes after cellularization. In the control (G), myosin is seen along the entire apical surface of the posterior midgut (between arrowheads) and at the junctions of cells beyond this region. In *fog* mutants (I), apical myosin is severely disrupted occurring in only a few isolated cells underlying the pole cells (arrows). (H,J) Cross-sections showing anti-myosin II antibody staining along the apical surface of the ventral furrow (between arrowheads) in control OreR embryos (H) and in *fog* mutants (J), in which it is present in some cells (+) but not others (-).

pathways that control cell shape change in these cells (Costa et al., 1994) and/or a small maternal contribution of *fog*.

To determine whether *fog* is not only necessary but also sufficient to localize myosin to the apical side of cells we have made a *UASfog* transgene (see Materials and methods). Despite high levels of *fog* expression from this transgene during cellularization (Fig. 2A-F), there is no apparent change in myosin localization. Myosin localizes normally to the cellularization front and the subsequent basal loss of myosin in the ventral most cells and the increased depth of cellularization in these cells that occurs in normal embryos also occur in these *fog*-overexpressing embryos (Fig. 2G,J,M).

The first effects of *fog* expression are seen at the onset of gastrulation. In embryos uniformly expressing *fog* the apical localization of myosin now occurs in all cells instead of being restricted to a ventral domain (Fig. 2H,K,N). In the ventral cells of these *fog*-overexpressing embryos, the apical localization of myosin precedes the apical localization in the more lateral and dorsal cells and reaches a higher level. It is also a higher level than in the ventral cells of control embryos. It is unclear whether this reflects higher levels of *fog* expression in the ventral cells (owing to both endogenous and *UASfog* expression) or whether it reflects an earlier or increased competence of these ventral cells to react to *fog* signal. The apical localization of myosin in the lateral and dorsal cells of *fog*-overexpressing embryos continues throughout gastrulation (Fig. 2L,L,O) and occurs without any concomitant reduction in levels of basally localized myosin (Fig. 2N,O). This raises the possibility that the apical and basal localizations of myosin may be independently controlled.

Not all *fog*-overexpressing embryos show the same degree of ectopic apical myosin localization in lateral and dorsal cells. Furthermore, limited apical myosin staining is occasionally seen in control embryos. We quantified this variability over five separate experiments. During cellularization, onset of gastrulation and later gastrulation 0% ($n=54$), 73% ($n=66$) and 84% ($n=25$) of *fog*-overexpressing embryos show ectopic apical myosin compared with 0% ($n=33$), 8% ($n=26$) and 22% ($n=23$) of controls respectively.

In wild-type embryos myosin accumulates apically in all cells after the completion of ventral furrow invagination, at the onset of germ band extension (Bertet et al., 2004; Zallen and Wieschaus, 2004). Therefore, apical accumulation of myosin in dorsal and lateral cells of apparently gastrulating embryos may occur as the result of a delay in ventral furrow formation. To investigate this possibility, we followed time-lapse movies of gastrulating embryos and examined morphology in precisely timed embryo collections. In both cases, we found a slight delay in the completion of ventral furrow formation in *fog*-overexpressing embryos compared with controls. In equivalently aged collections, only 32% ($n=82$) of control embryos were undergoing ventral furrow formation compared with 45% ($n=145$) of *fog*-overexpressing embryos. This implies that *fog*-overexpressing embryos take about 1.4 times longer to complete ventral furrow formation than control embryos. However, this is considerably less than the ~3.5 times delay that would be required to account for the large difference seen in apical myosin localization between the *UASfog*-expressing embryos and controls. Assuming that if the process were to take twice as long in *UASfog* embryos this would account for 50% of the embryos showing apical myosin simply

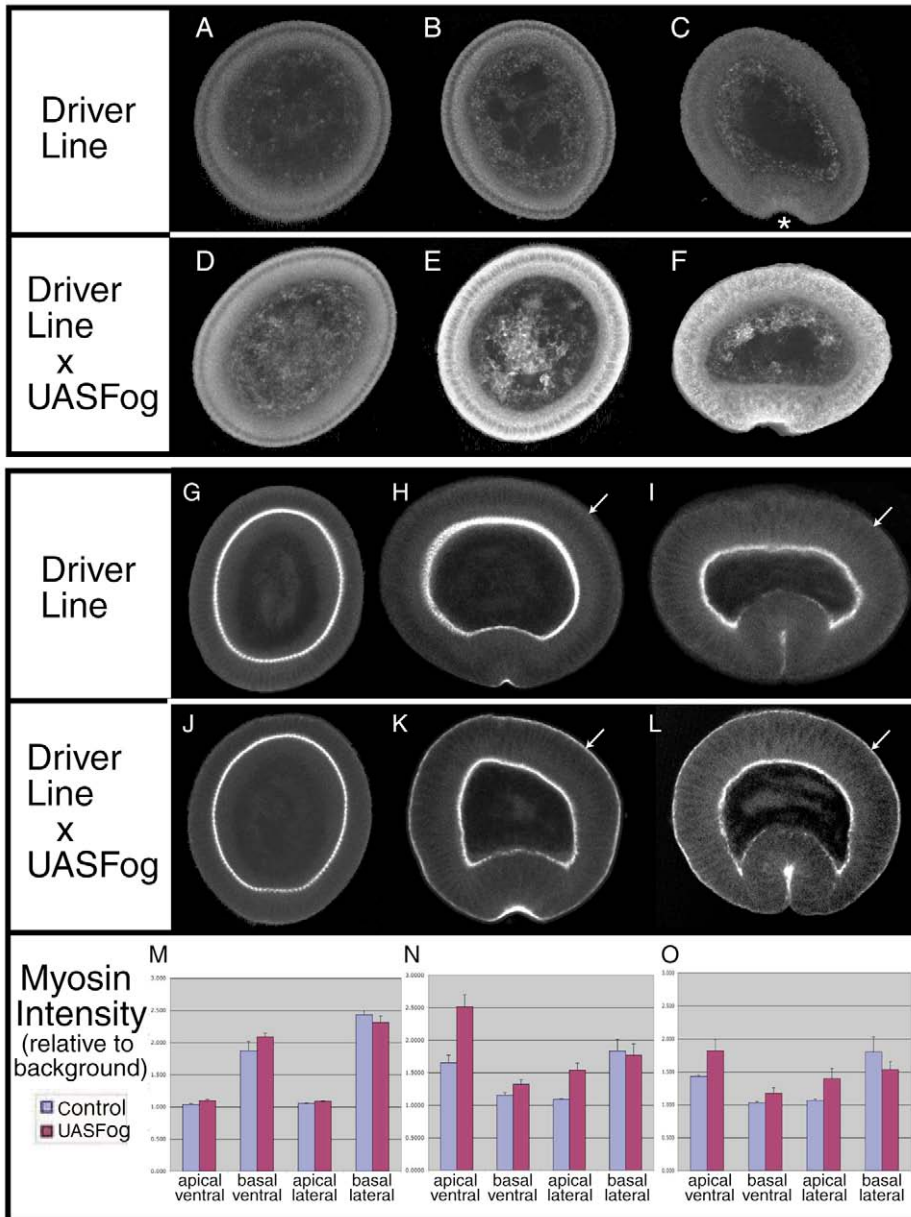


Fig. 2. Myosin localization in embryos misexpressing *fog*. (A-F) Staining for Fog protein in control embryos expressing just the *mat67;mat15* driver line (A-C) and this line driving *UASfog^b* expression (D-F). At the onset of cellularization (A,D), little *fog* expression is seen, but early in cellularization, before nuclear elongation (B,E), there is high *fog* expression throughout *UASfog* embryos. At the onset of gastrulation, there is low *fog* expression in the ventral furrow of control embryos (asterisk in C) and high expression throughout the *UASfog* embryos (F). (G-L) Control (G-I) and *UASfog*-expressing (J-L) embryos stained for myosin II. Myosin localizes normally to the basal cellularization front and decreases normally in ventral cells, which show the usual increase in cell depth (G,J). At the onset of gastrulation, myosin continues to be localized basally and now also localizes to the apical side of ventral cells in both control (H) and *UASfog* (K) embryos. Apical myosin is more intense in *UASfog* embryos and is no longer restricted to the ventral furrow, occurring in dorsal and lateral cells (arrow) too. This continues through later stages of gastrulation (comparing arrow in I and L). (M-O) Quantification of myosin intensity in driver-line control (blue) and *UASfog*-expressing (pink) embryos. Measurements were taken from the apical and basal sides of ventral and lateral cells at three different stages: (M) end of cellularization (see G,J), (N) onset of gastrulation (see H,K) and (O) later gastrulation (see I,L). No difference is seen between control and *UASfog* embryos at the end of cellularization (M) but during gastrulation (N,O) myosin increases on the apical side of both ventral and lateral cells in *UASfog* embryos with no corresponding decrease from the basal side. Error bars indicate s.e.m.

because they are in fact older, we estimate that the process would have to be ~ 3.5 times as long to account for the actual increased numbers of embryos we see (73% versus 8%).

Therefore *fog*-overexpressing embryos show a consistent increase in apical myosin staining in the lateral and dorsal cells of gastrulating embryos when compared with controls, and this increase is too large to be explained by the slight delay in gastrulation. We conclude that *fog* signaling is both necessary and sufficient to localize myosin II to the apical side of cells.

Functionally distinct modes of myosin localization

It is possible that *fog* provides a signal to localize or transport myosin apically, and myosin is then activated to interact and contract with actin. An intriguing alternative, however, is that *fog* itself may be activating myosin contractility, initiating an active motor-driven mechanism of myosin localization. To help distinguish between these two possibilities, we constructed a

form of myosin that is no longer able to interact or contract with actin and asked if this form of myosin was still able to localize normally.

Myosin is a hexamer comprising two myosin heavy chains (MHCs), two essential light chains and two regulatory light chains (RLCs). It is the globular head domain of the MHC subunits that interacts directly with actin and contains the region of ATPase activity that drives this actin-based motor. In addition the ATPase activity and strength of actin binding can be modified through phosphorylation of the regulatory light chains, while the coiled-coil tail domains of the MHCs are required for assembly of multiple myosin molecules into organized filaments (Tan et al., 1992).

We constructed a myosin-YFP transgene (mYFP-myosin Π^{DN}) in which the YFP moiety has replaced the actin-binding motor head domain of the myosin heavy chain, *zipper* (Fig. 3). Based on equivalent modifications in *Dictyostelium*, mYFP-

myosin II^{DN} homodimers should completely lack actin binding and contractility, and the ‘single headed’ wild-type myosin/mYFP-myosin II^{DN} heterodimers should have severely decreased actin binding and contractility (Burns et al., 1995; Uyeda and Yumura, 2000; Zang and Spudich, 1998). Consistent with this, we find that YFP-containing myosin isolated from mYFP-myosin II^{DN} expressing *Drosophila* embryos shows reduced actin binding when compared with wild-type myosin in a standard spin down assay (see Fig. S1 in the supplementary material). However, we do not detect any dominant-negative activity of this transgene during embryogenesis, presumably because of the high levels of endogenous myosin.

To analyze the localization of this mYFP-myosin II^{DN}, we used the Gal4 system to express the transgene uniformly in embryos that also carry wild-type copies of *zipper*. For comparison we examined: (1) a fully functional myosin-GFP fusion, in which GFP is fused to the myosin light chain, *sqhGFP* (Royou et al., 2004); and (2) the endogenous myosin II of wild-type embryos. We found no differences between the

localization patterns of *sqhGFP* and endogenous myosin, and herein refer only to the endogenous.

When cells divide during later stages of development, the non-functional mYFP-myosin II^{DN} (Fig. 3G) shows a localization similar to endogenous myosin (Fig. 3A). Both localize to the contractile ring as it forms, constricts and then disappears following the completion of cell cleavage. Similarly, during cellularization, we find that mYFP-myosin II^{DN} (Fig. 3H) localizes to the cellularization front in a manner similar to endogenous myosin (Fig. 3B). As previously reported for *sqhGFP* (Royou et al., 2004), the mYFP-myosin II^{DN} tends to form aggregates in the interior of the embryo (asterisk in Fig. 3H). In time-lapse movies, the aggregates associate with the cellularization front, which ‘clears’ them from the outer edges of the embryos as cellularization proceeds, but they do not fully integrate into the regular hexagonal array of mYFP-myosin II^{DN} associated with the advancing furrows (Fig. 3C,D).

The first differences between functional and non-functional myosin are observed at the onset of gastrulation. Unlike endogenous myosin (Fig. 3D), mYFP-myosin II^{DN} fails to

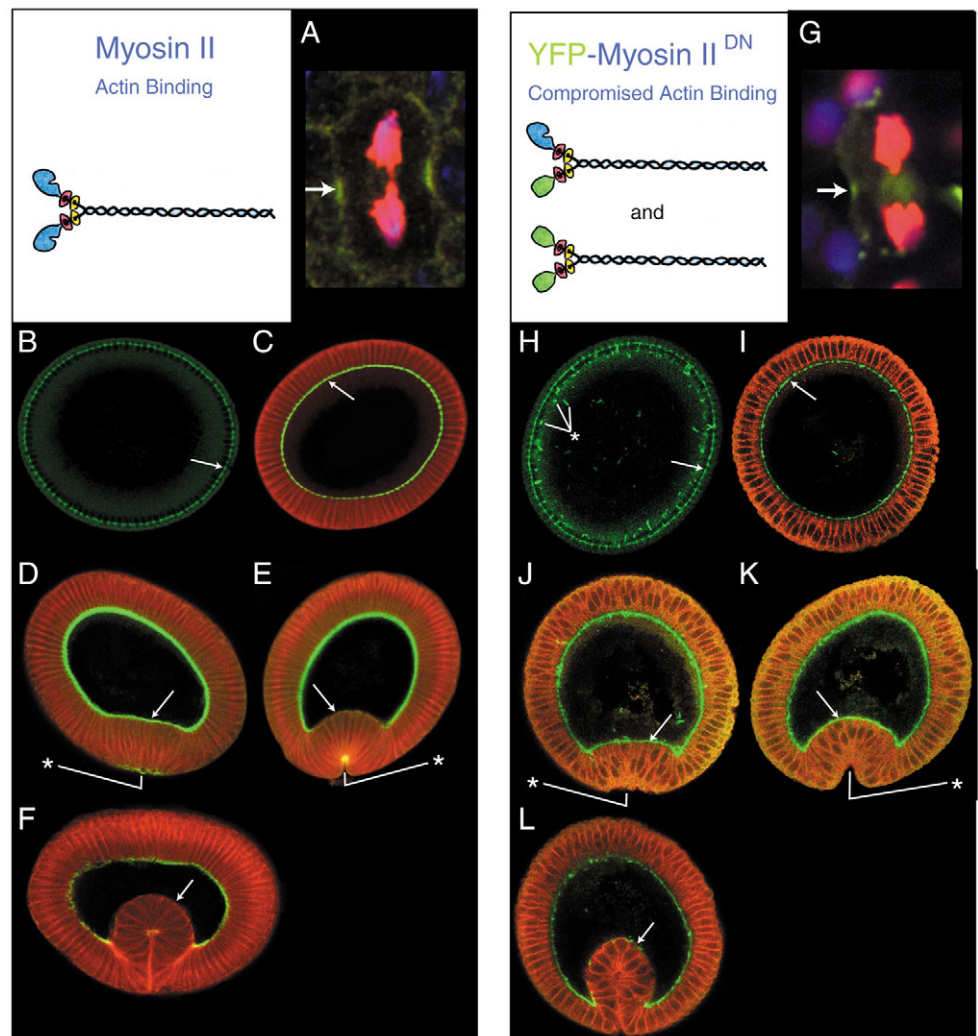


Fig. 3. Localization of non-actin binding YFP-Myosin II^{DN}. The schematic of myosin II structure shows the hexamer of two heavy chains (blue), two essential light chains (red) and two regulatory light chains (yellow). The schematic of mYFP-myosin II^{DN} shows the actin-binding head domain of the heavy chain replaced with the YFP moiety (green), resulting in two forms of YFP-containing myosin (heterodimer and homodimer) when expressed alongside endogenous myosin II, with both forms compromised in their ability to bind actin. (A,G) Cells undergoing cytokinesis are identified by antibody staining for phosphohistone H3 (red), nuclei are stained with Hoechst (blue) and myosin II (A) is stained with anti-myosin II antibody (green), whereas mYFP-myosin II^{DN} (G) is stained with anti-GFP antibody (green). Both myosin II and mYFP-myosin II^{DN} are localized to the cytokinetic furrow of dividing cells (arrow). (B-F,H-L) Anti-NRT staining (red), anti-myosin II staining (green in B-F) and anti-GFP staining (green in H-L). Despite the tendency of mYFP-myosin II^{DN} to form aggregates (asterisk in H), both the endogenous myosin II and the mYFP-myosin II^{DN} localize to the basal cellularization front (arrow in B,C,H,I), where levels later become greatly reduced in the ventral cells (arrow in F,L). This reduction is, however, delayed (E,K) and patchy (F,L) for mYFP-myosin II^{DN}. mYFP-myosin II^{DN} fails to

localize apically at the onset of ventral furrow formation (Fig. 3J) and throughout later stages of apical constriction (Fig. 3E,K) and invagination (Fig. 3F,L). The ability of these cells to undergo normal ventral furrow formation despite a lack of apically localized mYFP-myosin II^{DN} presumably reflects the activity of endogenous *zipper*. Both endogenous myosin and mYFP-myosin II^{DN} are lost from the basal side of the invaginating ventral furrow cells. This basal loss is slightly delayed (Fig. 3E,K) and patchy (Fig. 3F,L) for mYFP-myosin II^{DN}, but otherwise proceeds normally.

The requirement for actin binding and subsequent actin-dependent contractile activity therefore appears to distinguish two functionally different modes of myosin localization: an actin-independent mode of localization during cellularization and cytokinesis, and a second mode during gastrulation where localization to the apical side of the cell is dependent upon actin binding/contractility. It is possible that the mYFP-myosin II^{DN} is defective in ways other than its ability to interact with actin. However, equivalent constructs in *Dictyostelium* do not effect any other aspects of myosin function, including RLC phosphorylation or filament assembly (Burns et al., 1995; Uyeda and Yumura, 2000; Zang and Spudich, 1998). Therefore, although such secondary effects can not be entirely ruled out here, the defects seen are most likely a result of the inability to interact with actin and at the very least distinguish two different types of myosin localization to the apical and basal side of the cell. They also highlight the potential importance of actin-myosin interaction and contractility as a target for *fog* signaling.

RhoGEF, Rho-kinase and the *fog* pathway of myosin localization

The components acting downstream of *fog* to mediate its effects on the cytoskeleton are largely unknown. One candidate, RhoGEF2 (a guanine nucleotide exchange factor that promotes Rho activation) has been shown to be required for ventral furrow formation and can genetically interact with a *fog* transgene (Barrett et al., 1997; Hacker and Perrimon, 1998). However, embryos mutant for *RhoGEF2* have a much more severe disruption of ventral furrow formation than embryos mutant for *fog* and the point at which the products of these two genes interact on a mechanistic or subcellular level is unknown. Recent studies have shown a requirement for *RhoGEF2* in controlling actin dynamics/stability during cellularization (Grosshans et al., 2005; Padash Barmchi et al., 2005) and have also shown a disruption to myosin localization at gastrulation (Nikolaidou and Barrett, 2004). We therefore examined the re-localization of myosin during cellularization and gastrulation in *RhoGEF2* mutants and extended previous

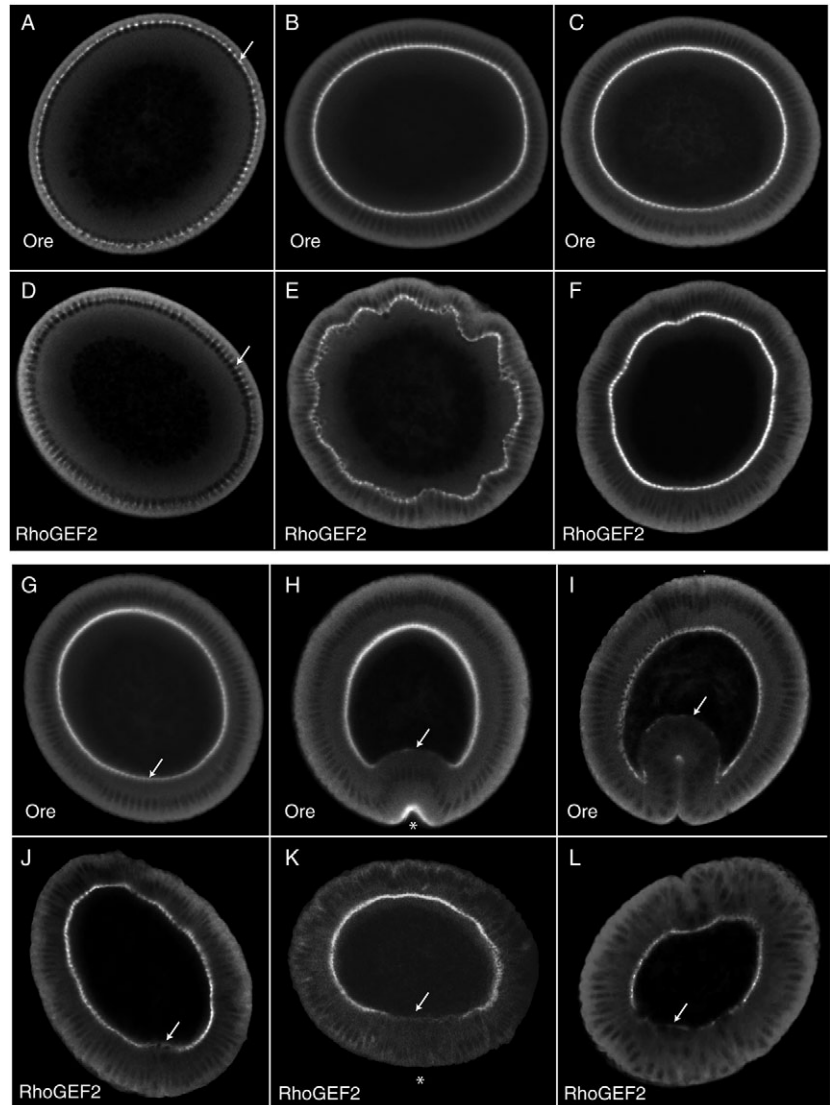


Fig. 4. Myosin localization in *RhoGEF2* mutant embryos. (A-F) Localization of myosin (white) to the cellularization front of Ore and *RhoGEF2* mutant embryos (arrow in A,D). The cellularization front of *RhoGEF2* mutant embryos is irregular at mid cellularization (E). (G-L) Localization of myosin during gastrulation. For precise staging, embryos were viewed under oil and individually fixed at the onset of gastrulation. Within this range of ages, 41% ($n=39$) of Ore embryos accumulate myosin on the apical side of ventral furrow cells (asterisk in H), but in *RhoGEF2* mutant embryos collected in the same way ($n=30$), myosin never accumulates apically above background levels (asterisk in K), whereas basal loss of myosin proceeds normally (arrow).

studies by looking at a potential downstream effector of *RhoGEF2* signaling.

Embryos mutant for *RhoGEF2* localize myosin normally to the forming cellularization front (Fig. 4A,D). However, unlike *fog* mutants, the *RhoGEF2* embryos show defects in cellularization including an irregular, wavy cellularization front (Fig. 4B,E). This implies that although RhoGEF2 function is not required to localize myosin to the cellularization front it is required to maintain the normal structure of the cellularization front and that the presence of myosin is not itself sufficient to maintain a straight

cellularization front. This is consistent with previous studies of *RhoGEF2* mutants and a potential role in controlling actin but not myosin dynamics (Grosshans et al., 2005; Padash Barmchi et al., 2005).

However, despite the defects during early cellularization, *RhoGEF2* mutant embryos that reach the end of cellularization look remarkably normal (Fig. 4C,F,G,J). The irregularity of the cellularization front recovers, particularly in the ventral cells, and both the increased cell depth and basal loss of myosin occur normally in these cells. However, in *RhoGEF2* embryos, precisely staged for the onset of gastrulation, there is an absolute failure to re-localize myosin to the apical side of the ventral cells (Fig. 4H,K), despite a normal loss of myosin from the basal side of these cells (Fig. 4H-L). This is consistent with independent mechanisms controlling the basal loss and apical accumulation of myosin during gastrulation and demonstrates an absolute requirement for RhoGEF2 in apical myosin localization. It also confirms the previous report of RhoGEF2 being required for apical myosin in ventral furrow cells (Nikolaidou and Barrett, 2004).

RhoGEF2 interacts with myosin in other systems through the Rho-kinase family of Ser/Thr kinases that inhibit myosin phosphatase and also directly phosphorylate myosin (Amano et al., 1996). Both these activities lead to activation of actin

binding by myosin and increased actomyosin based contractility. Additional myosin activators include MLCK and citron kinase but the extent to which these different activators play specific or overlapping roles with Rho-kinase is unclear (Matsumura et al., 2001), and the role of any of these myosin activators during *Drosophila* gastrulation is not known.

We therefore produced embryos mutant for *Drosophila Rho-kinase (Drok)* by making germline clones of two *Drok* alleles, both of which produced similar phenotypes. Myosin localizes to the cellularization front of *Drok* mutant embryos but often does so unevenly (Fig. 5A,D) and, as for *RhoGEF2*, the cellularization front is 'wavy' (Fig. 5E,F). Unlike the *RhoGEF2* mutant embryos, the nuclei of *Drok* mutant embryos have striking defects, including displacement into the interior of the embryo leaving reduced numbers at the cortex (Fig. 5D-F) and these remaining nuclei are often of increased size and irregular morphology (Fig. 5A-F). It is unclear to what extent these nuclear phenotypes may represent an earlier defect during cell-cycle/nuclear division.

Despite these defects, many *Drok* mutant embryos complete cellularization (Fig. 5F) and though the increased depth of cellularization in ventral cells is difficult to discern, basal loss of myosin proceeds normally (Fig. 5C,F,G,J). However, *Drok* mutant embryos show a complete failure to localize myosin to the apical side of the ventral cells at the onset of gastrulation ($n=14$) (Fig. 5F). At later stages of gastrulation, the outer layer of wild-type embryos consists of a single cell layered epithelium that folds in specific locations during germband extension (Fig. 5H). In *Drok* mutant embryos this morphology is severely disrupted and the outer epithelium becomes multilayered and irregular, containing large often rounded cells (Fig. 5K). *Drok* is therefore required to maintain epithelial integrity.

Both *Drok* and *RhoGEF2* mutant embryos show defects during cellularization and then fail to localize myosin to the apical side of ventral cells at gastrulation. However, it is unlikely that the earlier cellularization defects are what prevent the later apical myosin localization as many other cellularization mutants, such as *nullo*, display severe cellularization defects but still go on to localize myosin to the apical side of ventral cells at

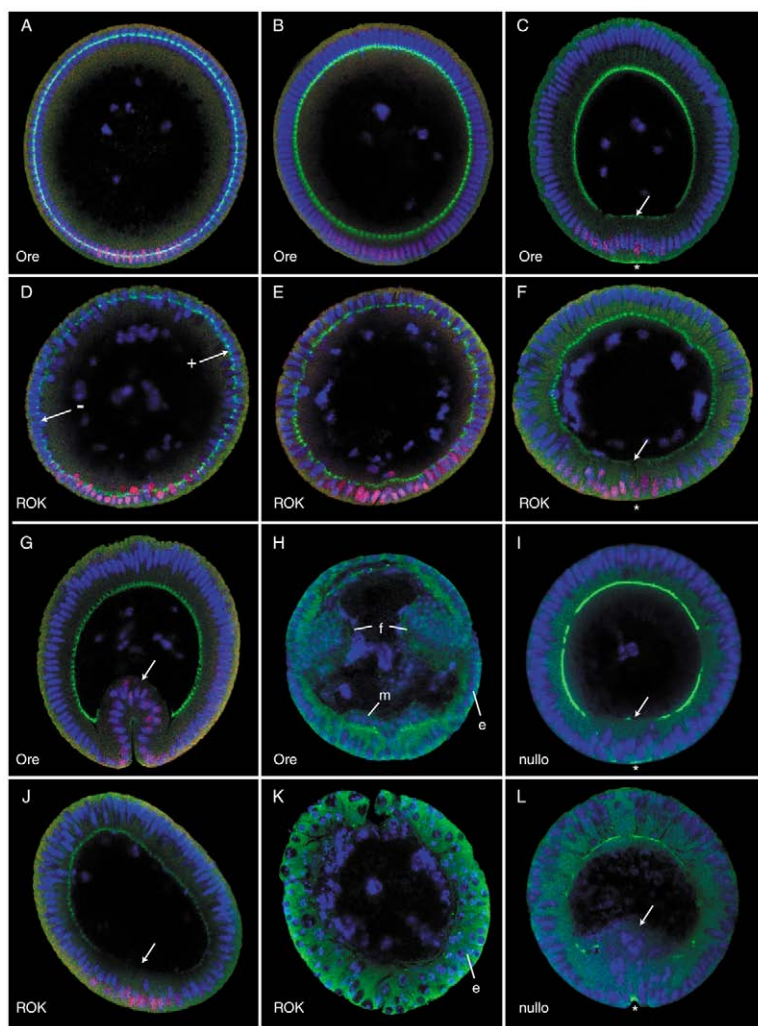


Fig. 5. Myosin localization in *Rho-kinase* mutant embryos. Staining for Dorsal protein (red) marks ventral cells, nuclei are Hoechst stained (blue) and anti-myosin II antibody staining is in green. (A-F) Myosin localization in control embryos (A-C) and equivalently staged *Rho-kinase* (ROK) mutant embryos (below, D-F). ROK embryos have irregular incorporation of myosin to the cellularization front (+, myosin present; -, reduced myosin incorporation), irregular nuclear morphology and a failure to localize myosin to the apical side of ventral cells at the onset of gastrulation (compare asterisk in C,F). (G-K) Control embryos (G,H) and ROK mutant embryos (J,K) at later stages of development. Cells in later ROK mutant embryos are irregular (K). e, epidermal cell layer; f, folds; m, mesodermal cell layer. (I,L) *nullo* mutant embryos show both basal loss (arrow) and apical localization of myosin (asterisk) in ventral cells at gastrulation (L), despite earlier cellularization defects (I).

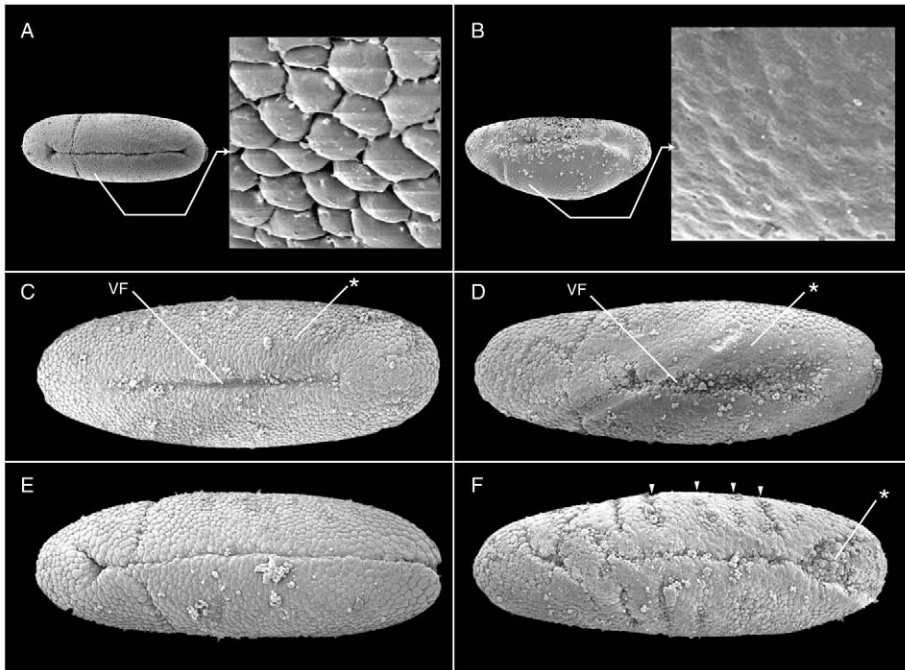


Fig. 6. The effects of *fog* signaling on cell surface morphology. Scanning electron micrographs of Ore-R (A,C,E) and *UASfog*-expressing (B,D,F) embryos. Inset shows the rounded apical surface of cells in Ore-R and the apical flattening seen in 23% ($n=21$) of embryos expressing *UASfog*¹². (C,D) Embryos expressing the stronger line, *UASfog*⁶, show disrupted, irregular, delayed ventral furrow formation (VF) and regions of apical flattening (asterisk) compared with Ore-R. (E,F) At the onset of germband extension, cells that fail to be internalized round up (asterisk) and lateral folds appear (arrowheads) in *UASfog*⁶-expressing embryos.

the onset of gastrulation (Fig. 5I,L). The failure of *Drok* and *RhoGEF2* mutant embryos to localize myosin apically during gastrulation therefore probably reflects a direct requirement for both these genes in the apical localization of myosin. Despite these disruptions to gastrulation, *Drok* embryos do still produce *fog* protein that is as punctate and apically concentrated as in wild-type embryos (Fig. 1F). This is therefore consistent with a model whereby *Drok* driven activation of myosin contractility drives myosin apically in response to *fog* and *RhoGEF2* signaling.

Translating myosin localization into cell shape change – the role of adherens junctions

To examine the morphological consequences of *fog*-induced myosin re-localization, we performed scanning electron microscopy (SEM) on embryos overexpressing *fog*. We see a range of phenotypes (Fig. 6) consistent with previous reports in which *fog* was expressed from a heat-shock promoter (Morize et al., 1998). It is difficult to predict the types of defects to expect in *fog* overexpressing embryos, as ventral furrow cells already express *fog* and cells outside the ventral furrow may require additional factors for full shape changes. Furthermore, early defects may lead to non-specific later defects by the end of gastrulation (Fig. 6F). However, apical flattening is the very first effect we see (Fig. 6B), coincident with the apical re-localization of myosin and this raises the issue of how these two processes are connected.

This connection is likely to require adherens junctions that anchor the actin-myosin cytoskeleton to the cell membrane and hold the cells of an epithelium together. Previous studies have concentrated on the role of junctions in cell polarity and maintaining integrity of epithelial sheets, or in cell rearrangements that do not involve changes in cell shape (Bertet et al., 2004; Tepass et al., 2001). Much less is understood about the role of adherens junctions in specific aspects of cell shape change.

We therefore analyzed the behavior of adherens junctions in *fog*-overexpressing embryos. At the completion of cellularization the embryo consists of a single layered epithelium with the basal junctions of cellularization located just apical to the myosin rich cellularization front and the newly forming adherens junctions located about 6 μm in from the apical surface of the embryo (Fig. 7A). At the onset of ventral furrow formation, adherens junctions in the ventral most region of the embryo shift to a completely apical location as the cell surfaces flatten, whereas the junctions in more lateral cells maintain their sub-apical position (Fig. 7B). These relative positions are maintained during the phase of apical constriction (Fig. 7C) as basal junctions gradually disappear. When *fog* is expressed throughout the embryo the apical shift of adherens junctions occurs normally in the ventral region (Fig. 7D,F), but now also occurs in more lateral and dorsal cells (Fig. 7E,G) and these junctions are more tightly condensed than the equivalent junctions of control embryos (Fig. 7G). The apical localization of myosin seen in *fog*-overexpressing embryos therefore correlates with an apical shift in adherens junctions.

The adherens junctions are possibly being pulled into an apical position because of forces generated by contractile myosin that has been apically re-localized in response to *fog* signal. To investigate the connection between myosin contractility and adherens junctions, we looked at myosin localization in embryos that lack adherens junctions.

It is not possible to examine embryos totally lacking junctional components such as Armadillo (Arm) as the maternally supplied components are required earlier during oogenesis. To get around this problem we have made use of the effects of *nullo* protein. Expression of *nullo* during late cellularization completely blocks the formation of apical spot junctions (Hunter et al., 2002; Hunter and Wieschaus, 2000). To confirm that results using this technique are due to the lack of adherens junctions and not to additional effects of *nullo*

expression we repeated the analysis with embryos made from *arm*^{043A01} germline clones. The *arm*^{043A0} allele is of the ‘medium class’ of *arm* alleles, lacking the last few Arm repeats and the entire C terminus. Germline clones of this class of alleles produce sufficient levels of Arm function to enable a few eggs to complete oogenesis but subsequent function of Arm in the embryo is severely compromised and these embryos fail to assemble apical adherens junctions (Cox et al., 1996; Tolwinski and Wieschaus, 2004). We find the same results using both techniques.

In both cases, myosin localizes normally to the basal cellularization front (Fig. 7H) (A. Sokac, unpublished) and to the apical surface of cells in the ventral furrow (Fig. 7I,J). This implies that functional Arm-containing junctions are not required for myosin to become localized within the cell. However, subsequent events are affected. As ventral furrow cells of wild-type embryos undergo apical constriction, myosin is seen throughout the apical surface of cells (Fig. 7K) but in embryos lacking junctions to tether the actin-myosin network myosin appears to contract into the center or side of the cell forming a tight ‘ball’ of presumably contracted myosin (Fig. 7L,M). The most likely explanation of these results is that myosin contractility is normal in cells lacking adherens junctions but when myosin is no longer tethered to junctions it contracts without being able to exert force on the plasma membrane. As a result, these cells are unable to flatten or constrict their apical surfaces. These results suggest that apically localized myosin is contractile and that this contractility alone is not sufficient to result in changes in cell shape but must be tethered to the apical adherens junctions to elicit apical flattening and constriction.

Adherens junctions are also known to play an important role in establishing and maintaining apicobasal polarity in epithelial cells (Nelson, 2003). However, our results demonstrate that the polarizing signal for the apical activation of myosin is not dependent upon any polarizing influence emanating from intact apical adherens junctions. This is consistent with the idea that it is the Fog protein, through its apical secretion and reception, that provides the polarizing signal for myosin activation and that this process is independent of intact adherens junctions.

Discussion

A new understanding of *fog* function

Previous studies had clearly demonstrated a requirement for *fog* in the process of apical flattening and constriction during ventral furrow and posterior midgut

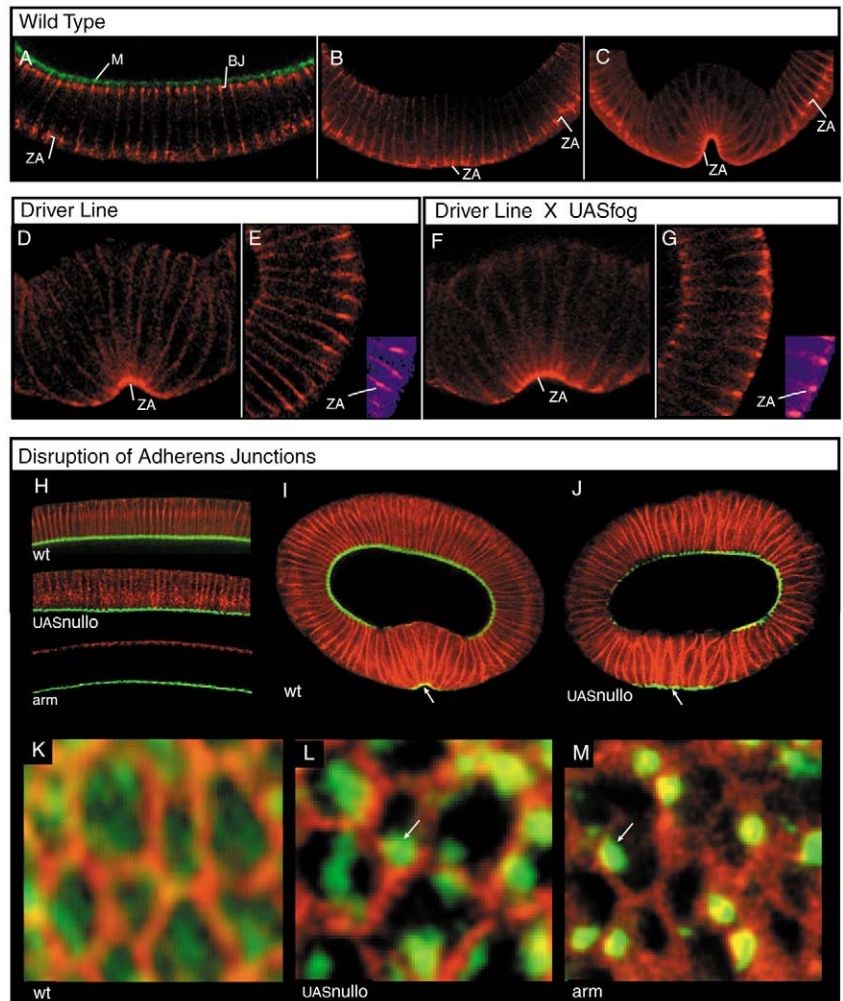


Fig. 7. The role of adherens junctions in response to *fog* signaling. (A-G) Staining of ventral (A-D,F) or lateral (E,G) cells showing the position of adherens junctions (zona adherens, ZA) and basal junctions (BJ) stained with anti-ARM antibody (red) and anti-myosin II antibody (M, green). (A-C) Movement of junctions in Ore-R embryos: ZA are located subapically in all cells at the end of cellularization (A) and this subapical position is maintained in lateral cells, while ZA move to the very apical edge of ventral cells at the onset (B) and during (C) gastrulation. (D,E) Control embryos from *mat67;mat15* mothers show the same dynamics of ZA movement as seen in Ore-R, with junctions located at the very apical edge of ventral cells (D) and subapically in lateral cells (E) and at the onset of gastrulation. (F,G) Embryos expressing *UASfog*⁶ from the *mat67;mat15* driver line show an apical shift of junctions in all cells both ventral (F) and lateral (G). Inset in E and G: non-specific background staining has been amplified in the blue channel to reveal the cell outline. (H-M) Localization of myosin II (green) to the cellularization front of wild-type embryos, and embryos in which junction formation has been disrupted (by expression of *UASnullo*, or by germline clone reduction of *arm* protein). Neurotactin staining is shown in red (except the *arm* panel in H where red staining is non-specific cell surface stain). (H) Myosin localizes normally to the cellularization front of wild-type, *UASnullo* and *arm* germline clone embryos. (I,J) Myosin localizes normally to the apical surface of ventral cells (arrow) at gastrulation in wild-type (I) and *UASnullo* (J) embryos. (K-M) Images of the apical surface of ventral cells. Cells are outlined by *Nrt* staining (red). Myosin (green) is localized throughout the apical surface of wild-type cells (K) but is constricted to a tight ball (arrow) within the cells of *UASnullo* (L) and *arm* germline clones (M), leaving large black (non-stained) areas without myosin that are not seen in wild type.

formation (Costa et al., 1994; Morize et al., 1998). Here, we extend these observations to identify molecular components of

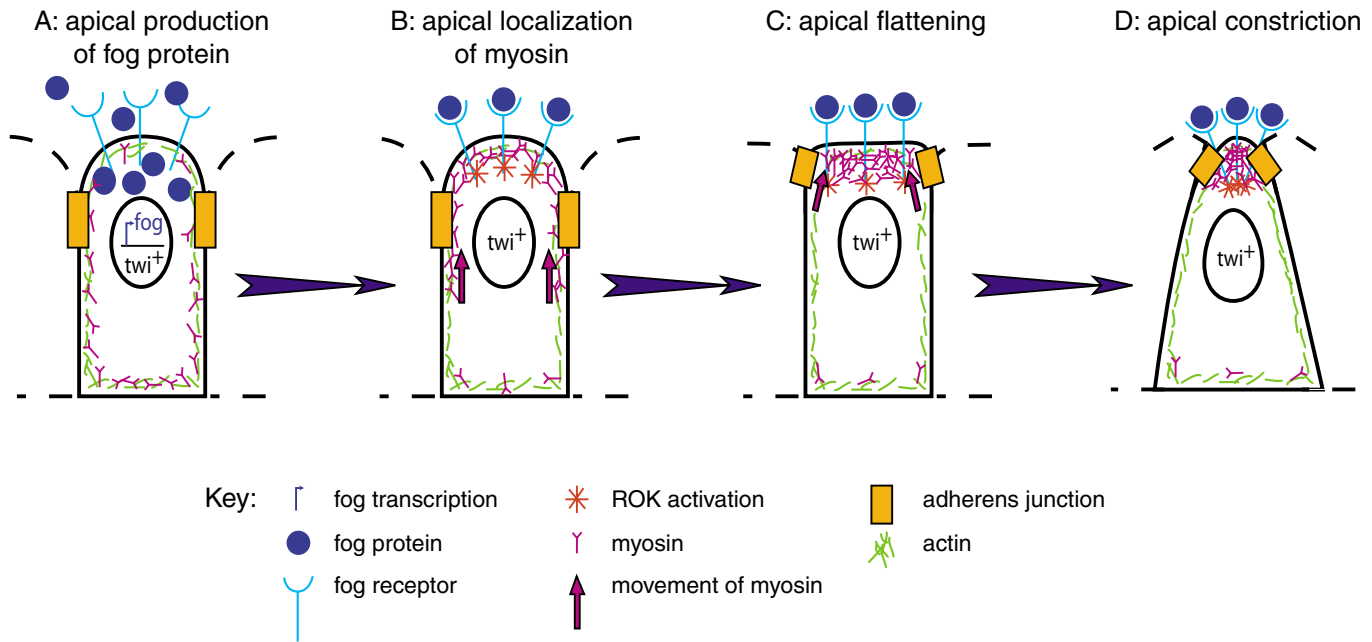


Fig. 8. Model of *fog* function in controlling cell shape change. (A) The patterning gene *twist* (*twi*), a transcription factor, specifies mesodermal fate of the ventral cells. As a consequence of *twi* expression, these cells activate transcription of *fog* (arrow), resulting in the production and secretion of *fog* protein from the apical side of the cell (blue dots). (B) Reception of *fog* signal on the apical side of the cell results in localized activation of ROK (red asterisk) which in turn activates the contractility of myosin with actin. This local source of actomyosin contractility drives myosin (pink) to the apical side of the cell (arrows). (C) The actin-myosin cytoskeleton is tethered to the cell surface through adherens junctions (orange). The force generated by apically localized contraction of the actin-myosin cytoskeleton therefore pulls down and flattens the domed apical cell surface and draws the adherens junctions up to the apical edge of the cell (arrows). (D) The continued contraction of apical actin-myosin exerts further force on the adherens junctions, pulling them close together, and resulting in the apical constriction of the cells.

the cytoarchitecture that respond to *fog* signal and the mechanism of *fog*-induced cell shape change.

fog encodes a secreted molecule, and it has been proposed that a secreted signal might be used as a way of co-coordinating apical flattening and constriction across a field of cells (Costa et al., 1994). We demonstrate that *fog* signal is both necessary and sufficient to trigger the relocalization of myosin to the apical side of the cell. This raises the possibility that a secreted signal is used as a means of producing a polarized response. In this case, secreting a signaling molecule on the apical side of the cell could be used to ensure an apically localized response to that signal. In support of this model, we find that *fog* protein is indeed apically concentrated and therefore comprises the earliest apically polarized component of this pathway. It will be interesting to see if the *fog* independent, parallel pathway of apical myosin recruitment uses a similar mechanism.

We also demonstrate that apical myosin localization requires the ability of myosin to interact and/or contract with actin. Furthermore, we show that *fog* signaling results in a shift of adherens junctions from their usual apicolateral position to a more apical position and that these junctions are necessary to translate contractile forces into physical changes in cell shape.

Taken together these data provide us with the following model (Fig. 8). Expression of the patterning gene *twi* in the prospective mesoderm cells results in activation of *fog* transcription. The resulting *fog* protein is then secreted from the apical surface of the cells and this signal activates *fog* receptors. The degree to which this activation is paracrine

versus autocrine has yet to be determined. The apically activated receptors trigger a transduction pathway involving the G- α subunit, Concertina, and the Rho activator RhoGEF2. A downstream target of this pathway is Rho-kinase, which in turn activates the ability of myosin to interact and contract with actin in this sub-apical region of the cell. A localized source of activated actin-myosin contractility initiates an active motor-driven mechanism of myosin localization which concentrates contractile myosin to the apical side of the cell. This actin-myosin network is tethered to the cell surface through adherens junctions. Contraction of this network therefore puts tension on the junctions, pulling them into a completely apical location and flattening the domed apical surface in the process. Continued contraction exerts further tension and ultimately pulls the junctions together so much that the entire apical cell surface constricts. Intriguingly, RhoGEF2 protein can associate with the tips of microtubules in cultured cells (Rogers et al., 2004). The extent to which this may add to a polarization of the *fog* pathway during gastrulation and how this ties in with the above model will therefore be interesting avenues for further investigation. It will also be important to examine any changes to the actin and microtubule organization of these cells.

The effects of *fog* overexpression also reveal some interesting features of *fog* function. Rates of apical flattening show more variability with the *UASfog* construct than reported for heat-shock *fog* embryos (Morize et al., 1998). It is unclear whether this reflects a dose sensitivity of the *fog* signaling pathway or whether the heat shock itself produces certain

changes in cytoarchitecture that alter the ability of the cell to respond to *fog* signal. Furthermore, the *fog*-overexpressing embryos are already making significant levels of *fog* protein at the onset of cellularization but myosin localization during cellularization remains unaffected. It is only after the completion of cellularization that the embryo becomes receptive to *fog* signaling and apical myosin localization. The ventral cells are then more receptive than dorsolateral cells. The nature of this receptivity, whether it simply requires the timely transcription of an additional component of the signaling cascade or whether it reflects a more complex aspect of cell states will be interesting to determine.

Two distinct mechanisms of myosin localization

In the transition between the morphogenetic processes of cellularization and gastrulation, myosin localizes in an intriguing pattern. In the dorsal and lateral regions of the embryo, myosin is restricted to the basal side of the cells. However, in the ventral-most cells this myosin is lost basally and accumulates apically. At first glance, this pattern of myosin localization is suggestive of a functional link between the basal loss of myosin and its appearance apically. However, by closely following myosin dynamics throughout cellularization, we find that these two events are temporally separable (R.E.D.-H., unpublished), with decreased levels of basally localized myosin significantly preceding the appearance of myosin on the apical side of the cell.

Here, we show that not only can the basal loss and apical accumulation of myosin be temporally separated, they can also be functionally separated. In embryos that express the *fog* signal ubiquitously, myosin accumulates apically in all cells but the basal loss of myosin is still restricted to the ventral cells. This demonstrates that a loss of myosin from the basal side of the cell is not required to localize myosin to the apical side. Conversely, in embryos mutant for *RhoGEF2* we find that myosin fails to accumulate apically but does still decrease basally in the ventral cells. The source of apically localized myosin (e.g. unlocalized cytoplasmic pool versus de novo synthesis) will therefore be interesting to determine.

Further evidence for functional differences between apical and basal localization comes from the differing requirements for junctional components and actin binding. Embryos made from *arm* germline clones have significantly reduced levels of functional Arm to incorporate into the basal junctions during cellularization and the apical adherens junctions at gastrulation. However, myosin is still able to correctly localize to the cellularization front, and to the apical side of ventral cells, but in the absence of junctions subsequent aspects of apical myosin localization become abnormal. The untethered myosin appears to contract into a tight ball in the center of the cell and fails to mediate the cell shape changes of apical flattening and constriction. Finally, we demonstrate that a YFP-myosin fusion protein that is compromised in both its actin binding and contractility still localizes to the cellularization front but fails to localize apically at gastrulation. This implies a requirement for actin binding and/or contractility in the mechanism by which myosin localizes apically during gastrulation, but not for its correct localization basally during cellularization. The fact that this YFP-myosin localizes correctly to cytokinetic furrows indicates that both myosin localization during cellularization and cytokinesis are

mechanistically more closely related than the mechanisms of apical and basal myosin localization that co-exist in the same cells at the onset of ventral furrow formation.

Multiple pathways controlling ventral furrow formation

It has been proposed that multiple pathways contribute to ventral furrow formation during *Drosophila* gastrulation. The ventral furrow of *fog* mutant embryos is disrupted but does still form, presumably through a parallel pathway of cell shape change (Costa et al., 1994). Embryos expressing *fog* from a transgene show a genetic interaction with *RhoGEF2* during gastrulation (Barrett et al., 1997) but *RhoGEF2* mutant embryos show a much more severe ventral furrow phenotype than *fog* mutants (Barrett et al., 1997; Hacker and Perrimon, 1998). Inhibition of RhoA function at later stages of development has a wide range of phenotypic consequences including disruption of apically localized myosin (Bloor and Kiehart, 2002). Removal of *RhoGEF2* also lowers levels of apical myosin (Nikolaidou and Barrett, 2004), though the degree and mechanism of this effect are less clear. How these multiple pathways interact and combine to direct cell shape changes during ventral furrow formation has therefore been unclear.

Here, we demonstrate that *fog* signaling directs the localization of myosin to the apical side of the cell, but in embryos lacking *fog* many cells of the ventral furrow still localize myosin apically. The ability of these cells to localize myosin in the absence of *fog* reveals that the parallel, *fog*-independent pathway also functions to control the apical localization of myosin. Furthermore, we demonstrate that *RhoGEF2* is absolutely required for apical localization of myosin in all cells of the ventral furrow. The difference in apical myosin localization between *fog* and *RhoGEF2* mutants is consistent with the fact that embryos lacking *RhoGEF2* display more severe ventral furrow defects than *fog* mutants. These results therefore reveal that the *fog* pathway and the *fog*-independent pathway probably converge at the level of *RhoGEF2* signaling of apical myosin localization.

In addition, the phenotypes of embryos lacking the Rho effector Rho-kinase (*Drok*) were distinct from those of *RhoGEF2* mutant embryos. Although both genes are required for apical myosin localization during gastrulation, the *Drok* embryos have more severe cellularization defects than *RhoGEF2* and some of these defects (particularly those involving nuclear morphology and fall-out) may even precede cellularization. This result is consistent with the idea that the RhoGEFs involved in activating Rho signaling tend to show more specificity for individual processes than the effectors downstream of Rho.

Furthermore, our results indicate that the role of *RhoGEF2* signaling in the process of apical myosin localization is most likely through activation of actin-myosin binding/contractility. We show that the apical myosin pathway requires Rho-kinase, a *RhoGEF2* effector known to directly activate myosin contractility. We also show that apical myosin localization is blocked when myosin contractility is impaired and that *RhoGEF2* signaling is absolutely required for this contractility based form of myosin localization. Conversely, the form of myosin localization that is independent of myosin contractility (during cellularization) is also independent of *RhoGEF2*

signaling. Interestingly many mutant backgrounds that severely disrupt cellularization are still capable of localizing apical myosin in ventral cells at the onset of gastrulation (E.F.W., unpublished). This not only provides further evidence of the differences between these two mechanisms of myosin function, but also strengthens the significance of the RhoGEF2 results, as RhoGEF2 has only a mild cellularization phenotype but completely blocks apical myosin localization at gastrulation.

Parallels to other systems

Rho signaling has been shown to control myosin activation in a number of different systems from cytokinesis in *C. elegans* to stress fiber formation in vertebrates (Etienne-Manneville and Hall, 2002; Piekny and Mains, 2002; Ridley and Hall, 1992). A variety of different types of receptors have been shown to activate Rho signaling (Wetschurck and Offermanns, 2002) and one particularly important pathway of Rho activation is through guanine nucleotide exchange factors (RhoGEFs), which catalyze the exchange of GDP for GTP on Rho GTPases, thus activating them. Signaling from Rho through the effector Rho-kinase then results in phosphorylation of myosin RLC and this cascade has been conserved in a variety of morphogenetic processes in *Drosophila*, including dorsal closure and bristle orientation in the adult epidermis (Bloor and Kiehart, 2002; Mizuno et al., 2002; Tan et al., 2003; Winter et al., 2001). Our results during gastrulation expand the role of this signaling cascade in *Drosophila* to include activation of myosin contractility as a means of controlling the subcellular localization of myosin and draws interesting parallels to the activators of this cascade in other systems.

In vertebrate cells, lysophosphatidic acid (LPA) activates a G-protein-coupled receptor. The alpha subunit of this G protein is a member of the G-alpha_{12/13} subclass, signaling through which leads to activation of Lsc/p115RhoGEF and the downstream cascade of Rho and Rho kinase activities that lead to myosin activation and formation of stress fibers and focal adhesions (Kozasa et al., 1998; Sawada et al., 2002). An additional Rho effector acting in this pathway is Dia, the interactions of which with both actin and microtubules may play a role in mediating alignment of microtubules and microfilaments during stress fiber formation (Tsuji et al., 2002). In the *fog* ventral furrow pathway, a number of direct homologies can be drawn to the LPA pathway of vertebrates. *Fog* signaling is thought to involve the G-protein alpha subunit *cta*, which also belongs to the G-alpha_{12/13} subfamily, though the identity of the receptor is not known (Parks and Wieschaus, 1991). We show here that the pathway of myosin localization in the ventral furrow also involves *RhoGEF2*, a *Drosophila* homologue of Lsc/p115RhoGEF and that the consequence of this activation of Rho signaling, is the *Drok*-mediated activation/localization of myosin, just as seen in stress fiber formation. To extend this comparison further, it will be interesting to address the role of *Dia* in ventral furrow formation.

Interesting parallels can also be drawn to myosin regulation in Dictyostelium. Peculiarities of the situation in Dictyostelium (including the lack of a Rho homologue, the importance of heavy rather than light chain phosphorylation and the fact that cytokinesis can occur in the absence of certain aspects of myosin phosphorylation and function) have led to the suggestion that Dictyostelium has developed a very different

and derived system for regulating myosin activity (see Matsumura et al., 2001). Our results, however, highlight some striking similarities. A myosin-GFP fusion protein that disrupts the ability of the head domain of MHC to interact with actin has been produced in Dictyostelium and just as we have found in *Drosophila* this compromised form of myosin is still able to localize correctly during cytokinesis (Zang and Spudich, 1998) but is unable to do so during cAMP-activated chemotaxis (Levi et al., 2002). As in *Drosophila*, ventral furrow formation this cAMP activated chemotaxis involves recruitment of myosin to the cell cortex and is a G-protein-coupled process. Our results therefore raise the possibility of distinct mechanistic parallels between the myosin based morphogenetic processes of these two organisms. Understanding how the multiple pathways controlling myosin dynamics in *Drosophila* are integrated into a developmental context, including how they interface with one another, with their downstream effectors and with the upstream patterning genes that control cell fate, may therefore provide insights that will extend beyond *Drosophila* to a diverse range of myosin-based processes.

We thank all members of the Wieschaus and Schüpbach laboratories for helpful discussions. For kindly providing fly stocks and reagents, we thank David Mickle, Kathy Barrett, Anne Royou, Liqun Luo, the Bloomington *Drosophila* Stock Center, Ruth Stewart, Dan Kiehart, Jim Haseloff, Chris Field, Carlos Alonso, John Reinitz and the Developmental Studies Hybridoma Bank. For their advice and assistance, we thank Reba Samanta, Anna Sokac, Jen Zallen, Girish Deshpande, Joe Goodhouse, Nan Yao and Jane Woodruff. We thank reviewers of an earlier version of this manuscript for their helpful comments. This work was supported by the Howard Hughes Medical Institute and by National Institute of Child Health and Human Development grant 5R37HD15587 to E.W. and by a Helen Hay Whitney Foundation fellowship to R.E.D-H.

Supplementary material

Supplementary material for this article is available at <http://dev.biologists.org/cgi/content/full/132/18/4165/DC1>

References

- Amano, M., Ito, M., Kimura, K., Fukata, Y., Chihara, K., Nakano, T., Matsuura, Y. and Kaibuchi, K. (1996). Phosphorylation and activation of myosin by Rho-associated kinase (Rho-kinase). *J. Biol. Chem.* **271**, 20246-20249.
- Barrett, K., Leptin, M. and Settleman, J. (1997). The Rho GTPase and a putative RhoGEF mediate a signaling pathway for the cell shape changes in *Drosophila* gastrulation. *Cell* **91**, 905-915.
- Barros, C. S., Phelps, C. B. and Brand, A. H. (2003). *Drosophila* nonmuscle myosin II promotes the asymmetric segregation of cell fate determinants by cortical exclusion rather than active transport. *Dev. Cell* **5**, 829-840.
- Bertet, C., Sulak, L. and Lecuit, T. (2004). Myosin-dependent junction remodelling controls planar cell intercalation and axis elongation. *Nature* **429**, 667-671.
- Bloor, J. W. and Kiehart, D. P. (2002). *Drosophila* RhoA regulates the cytoskeleton and cell-cell adhesion in the developing epidermis. *Development* **129**, 3173-3183.
- Brand, A. H. and Perrimon, N. (1993). Targeted gene expression as a means of altering cell fates and generating dominant phenotypes. *Development* **118**, 401-415.
- Burns, C. G., Larochelle, D. A., Erickson, H., Reedy, M. and De Lozanne, A. (1995). Single-headed myosin II acts as a dominant negative mutation in Dictyostelium. *Proc. Natl. Acad. Sci. USA* **92**, 8244-8248.
- Chen, M. S., Obar, R. A., Schroeder, C. C., Austin, T. W., Poodry, C. A., Wadsworth, S. C. and Vallee, R. B. (1991). Multiple forms of dynamin are encoded by shibire, a *Drosophila* gene involved in endocytosis. *Nature* **351**, 583-586.

- Chou, T. B. and Perrimon, N.** (1992). Use of a yeast site-specific recombinase to produce female germline chimeras in *Drosophila*. *Genetics* **131**, 643-653.
- Costa, M. R.** (1994). Cellular and molecular mechanisms controlling morphogenetic movements of gastrulation in *Drosophila*. PhD Thesis, Princeton University, Princeton, USA. 102 pp.
- Costa, M., Wilson, E. T. and Wieschaus, E.** (1994). A putative cell signal encoded by the folded gastrulation gene coordinates cell shape changes during *Drosophila* gastrulation. *Cell* **76**, 1075-1089.
- Cox, R. T., Kirkpatrick, C. and Peifer, M.** (1996). Armadillo is required for adherens junction assembly, cell polarity, and morphogenesis during *Drosophila* embryogenesis. *J. Cell Biol.* **134**, 133-148.
- Etienne-Manneville, S. and Hall, A.** (2002). Rho GTPases in cell biology. *Nature* **420**, 629-635.
- Glotzer, M.** (2001). Animal cell cytokinesis. *Annu. Rev. Cell Dev. Biol.* **17**, 351-386.
- Gonzalez-Gaitan, M.** (2003). Signal dispersal and transduction through the endocytic pathway. *Nat. Rev. Mol. Cell Biol.* **4**, 213-224.
- Grosshans, J., Wenzl, C., Herz, H. M., Bartoszewski, S., Schnorrer, F., Vogt, N., Schwarz, H. and Muller, H. A.** (2005). RhoGEF2 and the formin Dia control the formation of the furrow canal by directed actin assembly during *Drosophila* cellularisation. *Development* **132**, 1009-1020.
- Hacker, U. and Perrimon, N.** (1998). DRhoGEF2 encodes a member of the Dbl family of oncogenes and controls cell shape changes during gastrulation in *Drosophila*. *Genes Dev.* **12**, 274-284.
- Haseloff, J.** (1999). GFP variants for multispectral imaging of living cells. *Methods Cell Biol.* **58**, 139-151.
- Hunter, C. and Wieschaus, E.** (2000). Regulated expression of nulls is required for the formation of distinct apical and basal adherens junctions in the *Drosophila* blastoderm. *J. Cell Biol.* **150**, 391-401.
- Hunter, C., Sung, P., Schejter, E. D. and Wieschaus, E.** (2002). Conserved domains of the Nulls protein required for cell-surface localization and formation of adherens junctions. *Mol. Biol. Cell* **13**, 146-157.
- Kiehart, D. P., Lutz, M. S., Chan, D., Ketchum, A. S., Laymon, R. A., Nguyen, B. and Goldstein, L. S.** (1989). Identification of the gene for fly non-muscle myosin heavy chain: *Drosophila* myosin heavy chains are encoded by a gene family. *EMBO J.* **8**, 913-922.
- Kozasa, T., Jiang, X., Hart, M. J., Sternweis, P. M., Singer, W. D., Gilman, A. G., Bollag, G. and Sternweis, P. C.** (1998). p115 RhoGEF, a GTPase activating protein for G α 12 and G α 13. *Science* **280**, 2109-2111.
- Levi, S., Polyakov, M. V. and Egelhoff, T. T.** (2002). Myosin II dynamics in *Dictyostelium*: determinants for filament assembly and translocation to the cell cortex during chemoattractant responses. *Cell Motil. Cytoskeleton* **53**, 177-188.
- Matsumura, F., Totsukawa, G., Yamakita, Y. and Yamashiro, S.** (2001). Role of myosin light chain phosphorylation in the regulation of cytokinesis. *Cell Struct. Funct.* **26**, 639-644.
- Mizuno, T., Tsutsui, K. and Nishida, Y.** (2002). *Drosophila* myosin phosphatase and its role in dorsal closure. *Development* **129**, 1215-1223.
- Morize, P., Christiansen, A. E., Costa, M., Parks, S. and Wieschaus, E.** (1998). Hyperactivation of the folded gastrulation pathway induces specific cell shape changes. *Development* **125**, 589-597.
- Muller, H. A. and Wieschaus, E.** (1996). armadillo, bazooka, and stardust are critical for early stages in formation of the zonula adherens and maintenance of the polarized blastoderm epithelium in *Drosophila*. *J. Cell Biol.* **134**, 149-163.
- Nelson, W. J.** (2003). Epithelial cell polarity from the outside looking in. *News Physiol. Sci.* **18**, 143-146.
- Nikolaidou, K. K. and Barrett, K.** (2004). A Rho GTPase signaling pathway is used reiteratively in epithelial folding and potentially selects the outcome of Rho activation. *Curr. Biol.* **14**, 1822-1826.
- Oda, H. and Tsukita, S.** (2001). Real-time imaging of cell-cell adherens junctions reveals that *Drosophila* mesoderm invagination begins with two phases of apical constriction of cells. *J. Cell Sci.* **114**, 493-501.
- Padash Barmchi, M., Rogers, S. and Hacker, U.** (2005). DRhoGEF2 regulates actin organization and contractility in the *Drosophila* blastoderm embryo. *J. Cell Biol.* **168**, 575-585.
- Parks, S. and Wieschaus, E.** (1991). The *Drosophila* gastrulation gene concertina encodes a G α -like protein. *Cell* **64**, 447-458.
- Perrimon, N., Smouse, D. and Miklos, G. L.** (1989). Developmental genetics of loci at the base of the X chromosome of *Drosophila melanogaster*. *Genetics* **121**, 313-331.
- Piekny, A. J. and Mains, P. E.** (2002). Rho-binding kinase (LET-502) and myosin phosphatase (MEL-11) regulate cytokinesis in the early *Caenorhabditis elegans* embryo. *J. Cell Sci.* **115**, 2271-2282.
- Rajagopalan, S., Wachtler, V. and Balasubramanian, M.** (2003). Cytokinesis in fission yeast: a story of rings, rafts and walls. *Trends Genet.* **19**, 403-408.
- Ramaswami, M., Krishnan, K. S. and Kelly, R. B.** (1994). Intermediates in synaptic vesicle recycling revealed by optical imaging of *Drosophila* neuromuscular junctions. *Neuron* **13**, 363-375.
- Ridley, A. J. and Hall, A.** (1992). The small GTP-binding protein rho regulates the assembly of focal adhesions and actin stress fibers in response to growth factors. *Cell* **70**, 389-399.
- Rogers, S. L., Wiedemann, U., Hacker, U., Turck, C. and Vale, R. D.** (2004). *Drosophila* RhoGEF2 associates with microtubule plus ends in an EB1-dependent manner. *Curr. Biol.* **14**, 1827-1833.
- Royou, A., Field, C., Sisson, J. C., Sullivan, W. and Karess, R.** (2004). Reassessing the role and dynamics of nonmuscle myosin II during furrow formation in early *Drosophila* embryos. *Mol. Biol. Cell* **15**, 838-850.
- Sahai, E. and Marshall, C. J.** (2002). ROCK and Dia have opposing effects on adherens junctions downstream of Rho. *Nat. Cell Biol.* **4**, 408-415.
- Sawada, K., Morishige, K., Tahara, M., Ikebuchi, Y., Kawagishi, R., Tasaka, K. and Murata, Y.** (2002). Lysophosphatidic acid induces focal adhesion assembly through Rho/Rho-associated kinase pathway in human ovarian cancer cells. *Gynecol. Oncol.* **87**, 252-259.
- Tan, C., Stronach, B. and Perrimon, N.** (2003). Roles of myosin phosphatase during *Drosophila* development. *Development* **130**, 671-681.
- Tan, J. L., Ravid, S. and Spudich, J. A.** (1992). Control of nonmuscle myosins by phosphorylation. *Annu. Rev. Biochem.* **61**, 721-759.
- Tepass, U., Tanentzapf, G., Ward, R. and Fehon, R.** (2001). Epithelial cell polarity and cell junctions in *Drosophila*. *Annu. Rev. Genet.* **35**, 747-784.
- Tolwinski, N. S. and Wieschaus, E.** (2001). Armadillo nuclear import is regulated by cytoplasmic anchor Axin and nuclear anchor dTCF/Pan. *Development* **128**, 2107-2117.
- Tolwinski, N. S. and Wieschaus, E.** (2004). A nuclear function for armadillo/beta-catenin. *PLoS Biol.* **2**, E95.
- Tsuji, T., Ishizaki, T., Okamoto, M., Higashida, C., Kimura, K., Furuyashiki, T., Arakawa, Y., Birge, R. B., Nakamoto, T., Hirai, H. et al.** (2002). ROCK and mDia1 antagonize in Rho-dependent Rac activation in Swiss 3T3 fibroblasts. *J. Cell Biol.* **157**, 819-830.
- Uyeda, T. Q. and Yumura, S.** (2000). Molecular biological approaches to study myosin functions in cytokinesis of *Dictyostelium*. *Microsc. Res. Tech.* **49**, 136-144.
- Wang, Y. L.** (2001). The mechanism of cytokinesis: reconsideration and reconciliation. *Cell Struct. Funct.* **26**, 633-638.
- Wetschreck, N. and Offermanns, S.** (2002). Rho/Rho-kinase mediated signaling in physiology and pathophysiology. *J. Mol. Med.* **80**, 629-638.
- Winter, C. G., Wang, B., Ballew, A., Royou, A., Karess, R., Axelrod, J. D. and Luo, L.** (2001). *Drosophila* Rho-associated kinase (Drok) links Frizzled-mediated planar cell polarity signaling to the actin cytoskeleton. *Cell* **105**, 81-91.
- Young, P. E., Pesacreta, T. C. and Kiehart, D. P.** (1991). Dynamic changes in the distribution of cytoplasmic myosin during *Drosophila* embryogenesis. *Development* **111**, 1-14.
- Zallen, J. A. and Wieschaus, E.** (2004). Patterned gene expression directs bipolar planar polarity in *Drosophila*. *Dev. Cell* **6**, 343-355.
- Zang, J. H. and Spudich, J. A.** (1998). Myosin II localization during cytokinesis occurs by a mechanism that does not require its motor domain. *Proc. Natl. Acad. Sci. USA* **95**, 13652-13657.